A Kinetic Analysis of the Inward Calcium Current in 108CC15 Neuroblastoma × Glioma Hybrid Cells

S. Hering[1], R. Bodewei[1], B. Schubert[1], K. Rohde[2] and A. Wollenberger[1]

1 *Central Institute of Heart and Circulation Research*
2 *Central Institute of Molecular Biology, Academy of Sciences of the GDR, 1115 Berlin-Buch, German Democratic Republic*

Abstract. The kinetics of activation and inactivation of the inward calcium current (I_{Ca}) in morphologically undifferentiated and differentiated neuroblastoma × glioma hybrid cells of the clone 108CC15 were studied by the suction pipette technique for internal perfusion and voltage clamping. Potassium currents were eliminated by internal perfusion of the cells with a K^+-free solution. Activation of I_{Ca} followed a sigmoidal time course and could reasonably be fitted by a m^2 relation. The kinetics of I_{Ca} inactivation were studied by analyzing the current inactivation during long depolarizing steps and by measuring the peak I_{Ca} as a function of the length of a prepulse. Both methods gave comparable results indicating that the I_{Ca} inactivation cannot be fitted by a single exponential. The I_{Ca} inactivation was fitted by a biexponential function. Neither the activation nor the inactivation of I_{Ca} were changed after morphological cell differentiation induced by treatment with dibutyryl cyclic AMP.

Key words: Voltage clamp — Suction pipette method — Nerve cells — Calcium current kinetics

Introduction

In a preceding communication (Bodewei et al. 1985) we reported that morphological differentiation of the two clonal mouse neuroblastoma × rat glioma hybrid cell lines 108CC5 and 108CC15 (NG108-15), induced by N^6-2′-0-dibutyryl adenosine-3′,5′-monophosphate (dibutyryl cyclic AMP), was associated with an increase in the densities of the inward sodium and calcium currents (I_{Na} and I_{Ca}), while the voltage dependence of these currents and the ion selectivity of the slow calcium channel remained unaltered. Also it was noted that the voltage dependence of the

Presented at the 2nd International Symposium on Ionic Channels and Membrane Receptors, 21—26 May 1984, Smolenice, Czechoslovakia

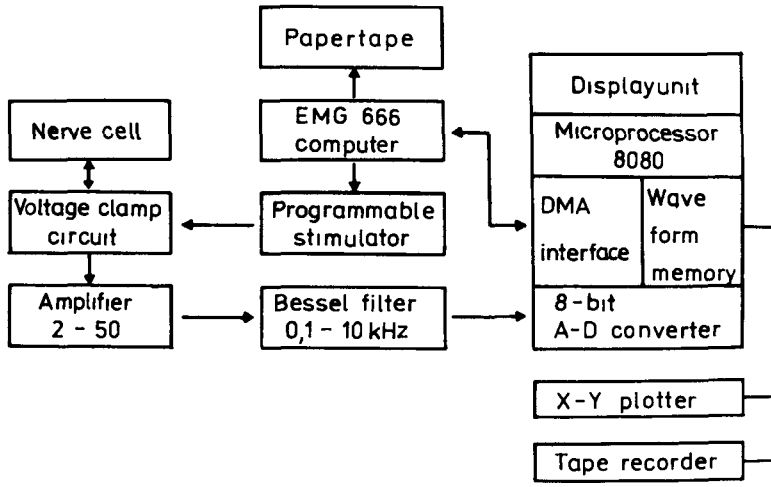

Fig. 1. Block diagram of the data recording system.

I_{Ca} and the selectivity of the Ca^{2+} channel were similar to what had been observed by Moolenaar and Spector (1978, 1979) in N1E-115 neuroblastoma cells.

In view of the crucial role played by I_{Ca} in the initiation and regulation of functional activities in neuroblastoma × glioma hybrid cells (Nirenberg et al. 1983) we felt that there was a need to know more about the properties of this ionic current. Accordingly we have undertaken an analysis of the kinetics of activation and inactivation of I_{Ca} in 108CC15 cells, which are the most extensively studied clone among the various neuroblastoma × glioma clonal hybrid lines.

Methods

The cells used were obtained by subculturing a batch of 108CC15 hybrids that was kindly donated by Prof. B. Hamprecht. They were cultured, internally perfused, and voltage clamped as described in the preceding paper (Bodewei et al 1985). For differentiation, which was monitored as morphological changes (see Bodewei et al. 1985), the cells were cultured for 6 to 8 days with 1 mmol/l dibutyryl cyclic AMP, generously supplied by Boehringer Mannheim GmbH. Undifferentiated cells in the exponential growth phase were used for comparison in some experiments.

The kinetic parameters of I_{Ca} were analyzed with the Wave Form Analyzer system 5500, EMG, Hungary. The command pulses and the recording of the current responses were controlled by an EMG-666 computer. Both the programmable X-Tal-controlled stimulator (EMG) and the Wave Form Analyzer system communicated with the computer through an interface (Fig. 1). The stimulator provided the pulse sequence to the voltage clamp and the sample commands to an 8 bit analog-to-digital converter.

The currents were digitized every 20 or 40 μs and 1 ms, respectively, for activation and inactivation analyses. The time constants of I_{Ca} activation and inactivation were determined from 4 averaged current

time recordings for a given voltage clamp step. For analysis of the I_{Ca} activation the current time course was corrected by subtraction of the linear component of the capacitative and leakage currents by averaging the current traces after hyperpolarizing and depolarizing voltage steps.

As a rule, about one hundred equally weighed data points were used for parameter estimation by equations (3) and (4) (see Results section) with the help of the nonlinear least squares curve fitting method of Marquardt as described by Reich et al. (1972), using a BESM-6 computer. The estimated variation range of the calculated τ_{h_1} and τ_{h_2} values was less than 5 and 20 per cent, respectively.

Results

Our kinetic analysis of I_{Ca} activation and inactivation in neuroblastoma × glioma hybrid cells is based on the Hodgkin-Huxley model (Hodgkin and Huxley 1952) with a modification describing the inactivation as a biexponential process.

The Ca^{2+} permeability is given by

$$P_{Ca} = \bar{P}_{Ca} \cdot m^n \cdot h, \text{ with } h = h_1 + h_2. \quad (1)$$

The potential and time-dependent Ca permeability coefficient P_{Ca} is defined by the constant-field relation (Fatt and Ginsborg 1958)

$$I_{Ca} = P_{Ca} \cdot \frac{4\ VF^2}{RT} \cdot \frac{[Ca]_i \exp(2\ VF/RT) - [Ca]_0}{\exp(2\ VF/RT) - 1}. \quad (2)$$

According to calculations taking into account $K_{D_{CaHPO_4}}$ and $K_{D_{HPO_4^{2-}}}$ of 50.12 l/mol and 10^{-7} mol/l, respectively, $[Ca]_i$ was calculated to be below 10^{-6} mol/l. F, R, and T have the usual thermodynamic meanings.

Activation of I_{Ca}

Fig. 2*A* shows the rising phase of the Ca^{2+} current in the neuroblastoma × glioma hybrid cells during different voltage steps after digital substraction of leakage and capacity currents. It can be seen that the activation of I_{Ca} follows a sigmoidal time course. The experimental points were fitted to

$$I_{Ca} = \bar{I}_{Ca} (1 - \exp(-t/\tau_m))^n \quad (3)$$

and corrected for inactivation after fitting the current decay to a biexponential function (see Methods). According to Fig. 2*A* the activation of the Ca current is reasonably fitted by a m^2 relation.

The activation time constant decreased from about 7 ms at −40 mV to 3.5 ms at 0 mV in undifferentiated as well as differentiated hybrid cells (Fig. 2*B*). The

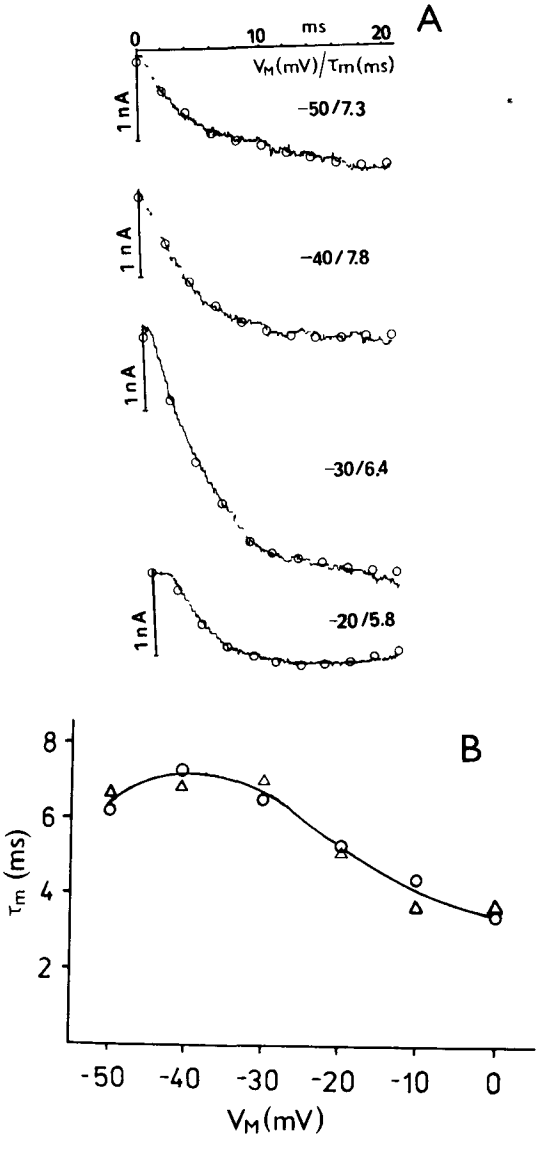

Fig. 2. (*A*) Calcium currents corrected for leakage and capacity currents (see Methods). The membrane potential is indicated for each trace. Circles (○) represent values yielded by equation (3) (see text) after activation (see text) after correction for inactivation. Holding potential −80 mV. (*B*) Relationship between I_{Ca} activation, τ_m, and voltage in undifferentiated (○) and differentiated (△) 108CC5 neuroblastoma × glioma hybrid cells (mean values of two cells each).

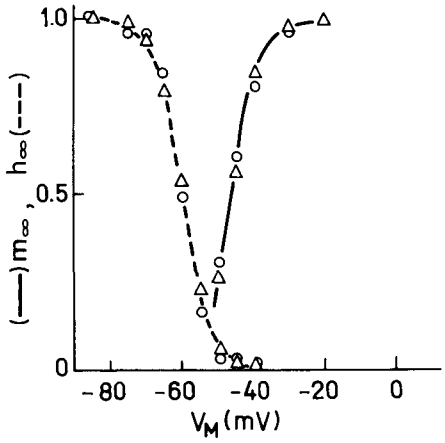

Fig. 3. Voltage dependence of steady state inactivation (dashed line) compared with that of the steady state activation of Ca permeabilities in undifferentiated (O) and differentiated (△) 108CC15 hybrid cells.

steady state activation of I_{Ca} (Fig. 3) is calculated from $m_{00} = \sqrt[2]{\frac{P_{Ca}}{\bar{P}_{Ca}}}$, the calcium permeabilities having been obtained from the maximum Ca^{2+} current at a given voltage step after correction for inactivation.

Inactivation of I_{Ca}

In all hybrid cells studied, the inactivation of I_{Ca} in the voltage range of −30 to +10 mV was not a single exponential function (Fig. 4*A*). The time course for inactivation can be expressed mathematically by the equation:

$$I_{Ca_{dec}} = A \exp(-t/\tau_{h_1}) + B \exp(-t/\tau_{h2}) + C, \quad (4)$$

where τ_{h1} and τ_{h2} represent the fast and slow time constants of the current inactivation, respectively. The values of τ_{h_1} and τ_{h_2} were obtained by a computer from the least squares fit of the I_{Ca} inactivation (see Methods). At long depolarizing test pulses (1 s) the τ_{h1} and τ_{h2} values obtained from a semilogarithmic plot of the I_{Ca} inactivation were comparable to those yielded by the least square fit of the function (Fig. 4*B*). At shorter test pulses, τ_{h_1} and τ_{h_2} could not be separated sufficiently by the linear method.

Like in myelinated nerve (Chiu 1977), the coefficients *A* and *B* are voltage dependent. The fast component of the amplitude became increasingly dominant

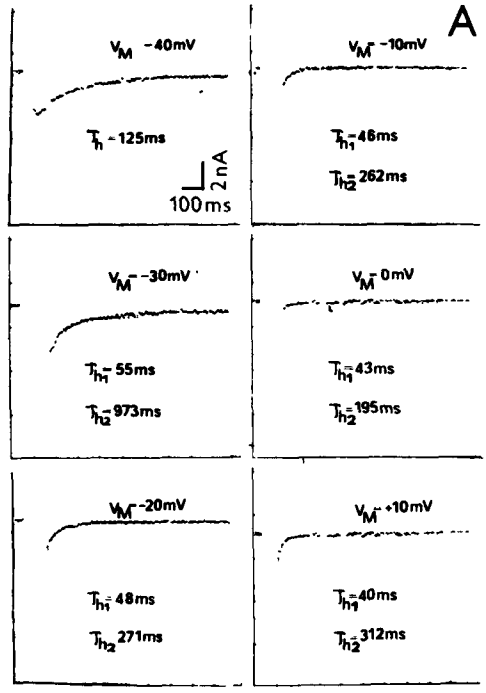
A
V_M -40mV
τ_h = 125ms
2 nA
100 ms
V_M = -10mV
τ_{h1} = 46ms
τ_{h2} = 262ms
V_M = -30mV
τ_{h1} = 55ms
τ_{h2} = 973ms
V_M = 0mV
τ_{h1} = 43ms
τ_{h2} = 195ms
V_M = -20mV
τ_{h1} = 48ms
τ_{h2} 271ms
V_M = +10mV
τ_{h1} = 40ms
τ_{h2} = 312ms

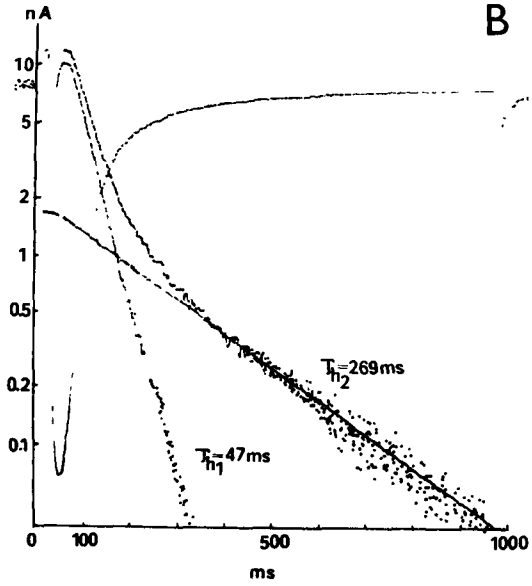
B
nA
10
5
2
1
0.5
0.2
0.1
0
100
500
1000
ms
τ_{h2} = 269ms
τ_{h1} = 47ms

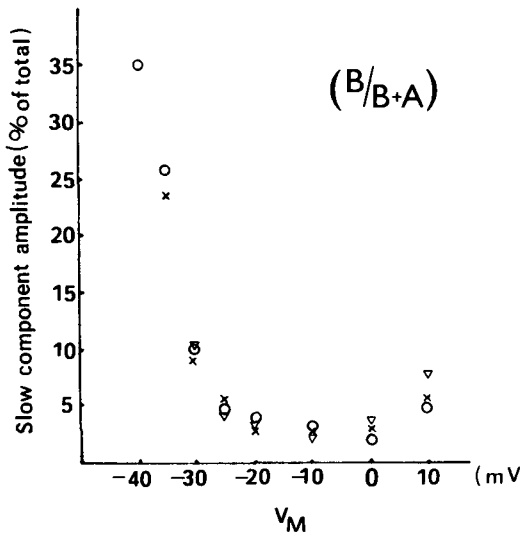

Fig. 5. Relative amplitude of the slow component (B/B + A) as a function of membrane potential in 3 different cells. The calcium concentration was 10 mmol/l (△), 19 mmol/l (○), and 50 mmol/l (×).

with increases in the test pulse amplitude and the slow component simultaneously decreased (Fig. 5). However, as shown in Fig. 5, the relative amplitude of the slow component at a given voltage was nearly the same in all cells studied.

The time constant of the fast inactivation of the I_{Ca} at different depolarizing potentials is shown in Fig. 6*A* and that of the slow inactivation for two extracellular Ca^{2+} concentrations is shown in Fig. 6*B*. Considering the shift in the *I*—*V* relationship induced by increasing the extracellular Ca^{2+} concentration (Fig. 6*B*) neither τ_{h_2} nor the voltage dependence of τ_{h_1} were affected by an increase in the current amplitude or by substitution of 10 mmol/l Ba^{2+} for 10 mmol/l Ca^{2+}.

As a second and independent method for the study of the voltage dependence of the I_{Ca} inactivation we used the double pulse method (Fig. 7*A*). When in the two

Fig. 4. (*A*) Inactivation of Ca^{2+} currents in a differentiated 108CC15 hybrid cell. V_M values indicate the membrane potential during 1-s pulses. We fitted the decay of the current by two exponentials, τ_{h_1} and τ_{h_2}, shown in each panel. At $V_M = -40$ mV the decay was fitted by a single exponential. The peak values of I_{Ca} in this particular experiment were slightly shifted in time because of low pass filtering. Scaling down on the upper left panel applies to all 6 panels. (*B*) Estimation of the inactivation time constants from the semilogarithmic plot of I_{Ca}. The straight line was fitted by microcomputer. The fast component was obtained by digitally subtracting the slow component from the whole inactivation time course. The curves and data points are photographs of the computer display.

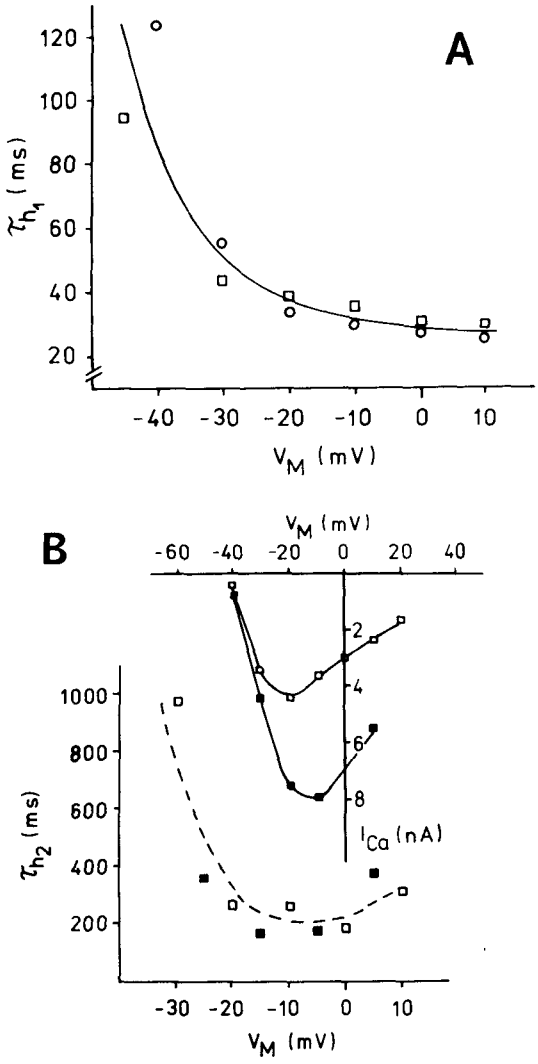

Fig. 6. (*A*) Time course of fast inactivation τ_{h_1} in undifferentiated (○) and differentiated (△) hybrid cells as a function of the membrane potential (mean values from 3 cells). (*B*). Time course of slow inactivation τ_{h_2} in differentiated 108CC15 cells as a function of membrane potential in 10 mmol/l $[Ca]_{out}$ (□) and 50 mmol/l $[Ca]_{out}$ (○). Inset shows the current-voltage relationship of I_{Ca} at the above two extracellular Ca^{2+} concentrations. Note the shift of I_{Ca} peak values. The time course of the slow inactivation was nearly the same in undifferentiated 108CC15 cells.

pulse experiments the logarithm of the test pulse current amplitude was plotted against the duration of the prepulse, the estimated time course could not be fitted by a single exponential (Fig. 7*B*). The estimated time constants of the fast and slow

components were found to be close to τ_{h1} and τ_{h2}. As observed from the decay of I_{Ca} for larger depolarizations the fast phase became dominant and the estimation of the second time constant was made difficult, since the slow component was closely approaching the zero line.

Discussion

I_{Ca} activation and inactivation in membranes of various nerve and muscle preparations (Henček and Zachar 1977; Akaike et al. 1978; Sanchez and Stefani 1978; Kostyuk et al. 1981; Llinás et al. 1981; Ashcroft and Stanfield 1982) could be fitted by the Hodgkin-Huxley model (1952) which assumes separate processes of activation and inactivation. For the present case, the original model needs to be expanded on the basis of the inactivation being a biexponential process.

As in snail neurons (Kostyuk et al. 1981; Byerly and Hagiwara 1982), I_{Ca} activation in the hybrid cells is reasonably well fitted by m^2 kinetics (Fig. 2*A*). However, according to more detailed studies of I_{Ca} activation kinetics in snail neurons (Brown et al. 1983) and chromaffin cells (Fenwick et al. 1982) an analysis that encompasses the tail currents is needed to obtain a full picture of I_{Ca} activation.

A biexponential time course of I_{Ca} inactivation has been described by several groups of investigators in neurons (Kostyuk and Krishtal 1977; Brown et al. 1981; Doroshenko et al. 1984) and other tissues (Ashcroft and Stanfield 1982; Isenberg and Klöckner 1982). In the present work, the kinetics of development of I_{Ca} decay was studied by two independent methods. With both the single and double pulse method the inactivation in the hybrid cells is better described by two time constants than it is by one. The fast and slow time constants of I_{Ca} inactivation were observed in differentiated as well as in undifferentiated hybrid cells. The values of both time constants were not significantly dependent on the I_{Ca} current amplitude (Fig. 6*B*). It therefore seems unlikely that series resistance can account for the observed nonexponential decay of the calcium current. The leakage current was always linear in the studied potential range. As reported in the preceding paper (Bodewei et al. 1985), nonspecific outward currents could be detected only during large depolarizing steps in the potential range more positive than +10 mV. All these facts indicate that, over a voltage range of −30 mV to +10 mV, where the nonexponential inactivation of I_{Ca} is most prominent, this decay should be attributed to I_{Ca} relaxation.

The determined fast and slow time constants of I_{Ca} inactivation in the hybrid cells are comparable to the I_f-and I_s-values of I_{Ca} decline determined by Doroshenko et al. (1984) in snail neurons. These authors attributed the fast decline of I_{Ca} to an activation of a nonspecific outward current. As pointed out above, this was certainly not the case in the present experiments at potentials more negative than

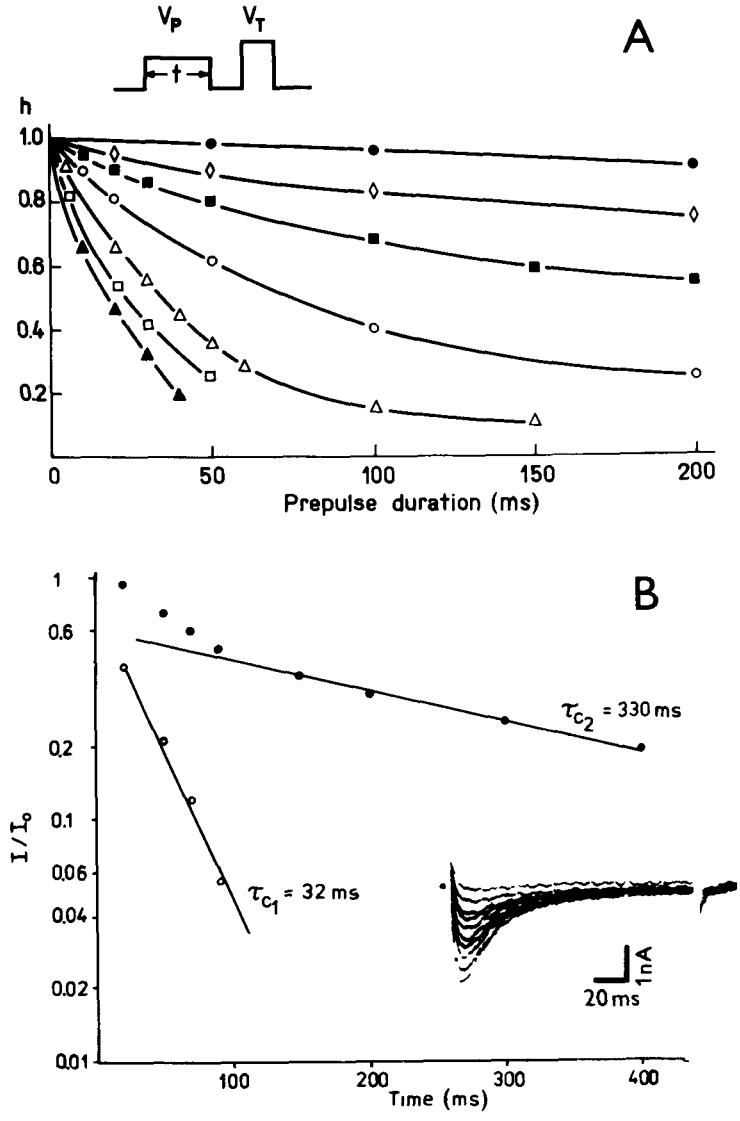

Fig. 7. (*A*) Turn-off of the calcium current in two-pulse experiments. Ordinate shows I_{Ca} (elicited by test pulse) relative to I_{Ca} without prepulse. Abscissa: duration of prepulse (ms). Test pulse duration 100 ms. Prepulse potentials (V_p) were from −50 to −10 mV for measurements of onset of inactivation. The curves for −50, −45, −35 and −30 mV could be fitted by the sum of two exponentials. At potentials positive to this range only one exponential could be determined (see text). Pulse protocol (see text) consisted of a prepulse and a test pulse to −30 mV, separated by a 40 ms interval. (●) 50 mV; (□) 45 mV; (■) 40 mV (○) 35 mV; (△) 30 mV; (□) 20 mV; (▲) 15 mV. (*B*). Data for prepulse

+10 mV. Neither did we observe a Ca^{2+}-dependent inactivation caused by entry of Ca^{2+} ions into the cell, as described by Brehm and Eckert (1977) and by Tillotson (1979).

Our kinetic analysis of I_{Ca} in 108CC15 neuroblastoma × glioma hybrid cells indicates that, with respect to its inactivation kinetics, this current is comparable to the Na^+ current in the node of Ranvier (Meves 1978). Studies of I_{Ca} in nerve cells of various species have revealed differences in phenomenological properties of this current that may reflect the existence of several types of Ca^{2+} channels (Hagiwara and Byerly 1981; Tsien 1983; Kostyuk, personal communication). In the present study, no significant change in the kinetic properties of I_{Ca} could be detected in the neuroblastoma × glioma hybrid cells after prolonged treatment with dibutyryl cyclic AMP, although the morphology of the cells, which had ceased to proliferate (Bodewei et al. 1985), was markedly changed.

The nonexponential decay of I_{Ca} in the present study was fitted by the sum of two exponentials. The reasonable fit of the experimental data by the proposed model could be interpreted as evidence for the existence of two Ca^{2+} channel populations with different inactivation properties. In analogy to Chiu's model of I_{Na} inactivation (Chiu 1977), a three state model may also fit the present data of a biexponential decay of I_{Ca} in the 108CC15 hybrid cells. Investigations on single channels can be expected to answer this question.

Acknowledgements. We thank Prof. B. Hamprecht for having kindly supplied us with 108CC15 cells. We also thank Boehringer Mannheim GmbH for a generous gift of dibutyryl cyclic AMP. Thanks are due to Dr. T. Rösner and Mr. W. Schälike for assistance in the mathematical treatment of the experimental data and to Holle Schmidt for valuable technical assistance.

potential of −40 mV plotted semilogarithmically. Inset: I_{Ca} during the test pulse. In general, curves could be fitted by an equation of the form

$$I(t) = A \exp(-t/\tau_{C1}) + B \exp(-t/\tau_{C2}),$$

where A and B are constants.

Using the results shown in the Figure 7A, τ_{C1} and τ_{C2} were calculated in 3 different cells to be at

$V_p = -50$ mV:	$\tau_{C1} = 312 \pm 48$ ms	and	$\tau_{C2} = 2020 \pm 300$ ms;
$V_p = -45$ mV:	$\tau_{C1} = 140 \pm 30$ ms	and	$\tau_{C2} = 1300 \pm 210$ ms;
$V_p = -35$ mV:	$\tau_{C1} = 61 \pm 19$ ms	and	$\tau_{C2} = 230 \pm 28$ ms;
$V_p = -30$ mV:	$\tau_{C1} = 29 \pm 3$ ms	and	$\tau_{C2} = 230 \pm 28$ ms;
$V_p = -20$ mV:	$\tau_{C1} = 27 \pm 4$ ms;		
$V_p = -15$ mV:	$\tau_{C1} = 21 \pm 6$ ms.		

References

Akaike N., Lee K. S., Brown A. M. (1978): The calcium current of *Helix* neuron. J. Gen. Physiol. **71**, 509—531

Ashcroft F. M., Stanfield P. R. (1982): Calcium inactivation in skeletal muscle fibres of the stick insect, *Carausius morosus*. J. Physiol. (London) **330**, 349—372

Bodewei R., Hering S., Schubert B., Wollenberger A. (1985): Sodium and calcium currents in neuroblastoma × glioma hybrid cells before and after morphological differentiation by dibutyryl cyclic AMP. Gen. Physiol. Biophys. **4**, 113—128

Brehm P., Eckert R. (1978): Calcium entry leads to inactivation of calcium channel in Paramecium. Science **202**, 1203—1206

Brown A. M., Morimoto K., Tsuda Y., Wilson D. L. (1981): Calcium current-dependent and voltage-dependent inactivation of calcium channels in *Helix aspera*. J. Physiol. (London) **320**, 193—218

Brown A. M., Tsuda Y., Wilson D. L. (1983): A description of activation and conduction in calcium channels based on tail and turn-on current measurements in the snail. J. Physiol. (London) **344**, 549—583

Byerly L., Hagiwara S. (1982): Calcium currents in internally perfused nerve cell bodies of *Limnea stagnalis*. J. Physiol. (London) **322**, 503—528

Chiu S. Y. (1977): Inactivation of sodium channels: second order kinetics in myelinated nerve. J. Physiol. (London) **273**, 573—596

Doroshenko P. A., Kostyuk P. G., Martynyuk A. E. (1984): Inactivation of calcium current in the somatic membrane of snail neurons. Gen. Physiol. Biophys. **3**, 1—17

Fatt P., Ginsborg B. L. (1958): The ionic requirements for the production of action potential in crustacean muscle fibres. J. Physiol. (London) **142**, 516—543

Fenwick M. E., Marty A., Neher E. (1982): Sodium and calcium channels in bovine chromaffin cells. J. Physiol. (London) **331**, 599—635

Hagiwara S., Byerly L. (1981): Calcium channel. Annu. Rev. Neurosci. **4**, 69—125

Henček M., Zachar J. (1977): Calcium currents and conductances in the muscle membrane of the crayfish. J. Physiol. (London) **268**, 51—71

Hodgkin A. L. Huxley A. F. (1952): A quantitative description of membrane current and its application to conduction and excitation in nerve. J. Physiol. (London) **117**, 500—544

Isenberg G., Klöckner U. (1982): Calcium currents of isolated bovine ventricular myocytes are fast and of large amplitude. Pflügers Arch. **395**, 30—41

Kostyuk P. G., Krishtal O. A. (1977): Effect of calcium and calcium-chelating agents on the inward and outward currents in the membrane of mollusc neurons. J. Physiol. (London) **270**, 569—580

Kostyuk P. G., Krishtal O. A., Pidoplichko V. I. (1981): Calcium inward current and related charge movements in the membrane of snail neurons. J. Physiol. (London) **310**, 403—421

Llinás R., Steinberg I. Z., Walton K. (1981): Presynaptic calcium currents in squid giant synapse. Biophys. J. **33**, 289—322

Meves H. (1978)): Inactivation on the sodium permeability in squid giant nerve fibres. Prog. Biophys. Molec. Biol. **33**, 207—230

Moolenaar W. H., Spector I. (1978): Ionic currents in cultured mouse neuroblastoma cells under voltage-clamp conditions. J.Physiol. (London) **278**, 265—286

Moolenaar W. H., Spector I. (1979): The calcium current and the activation of a slow potassium conductance in voltage-clamped mouse neuroblastoma cells. J. Physiol. (London) **292**, 307—323

Nirenberg M., Wilson S., Higashiola H., Rotter A., Krueger K., Rusis N., Ray R., Kenima J. G., Adler M. (1983): Modulation of synapse formation by cyclic adenosine monophosphate. Nature **222**, 794—799

Reich J. G., Wangermann G., Falck M., Rohde K. (1972): A general strategy for parameter estimation from isosteric and allosteric-kinetic data and binding measurements. Eur. J. Biochem. **26**, 368—379

Sanchez J. A., Stefani E. (1978): Inward calcium currents in twitch muscle fibres of the frog. J. Physiol (London) **283**, 197—209

Tillotson D. (1979): Inactivation of Ca conductance dependent on entry of Ca ions in molluscan neurons. Proc. Nat. Acad. Sci. USA **76**, 1497—1500

Tsien R. W. (1983): Calcium channels in excitable cell membranes. Annu. Rev. Physiol. **45**, 341—358

Zahradník I., Zachar J. (1982): Calcium currents in the muscle membrane of the crayfish in K^+-free internal environment. Gen. Physiol. Biophys. **1**, 457—461

Zahradník I., Zachar J. (1983): Inhibitory effect of verapamil upon calcium and potassium currents in crayfish muscle membrane. Gen. Physiol. Biophys. **2**, 181—192

Received May 29, 1984/Accepted July 22, 1984